Thin-Film Microsusceptometer With Integrated Nanoloop

Dietmar Drung, Jan-Hendrik Storm, Frank Ruede, Alexander Kirste, Marcel Regin, Thomas Schurig, Ana M. Repollés, Javier Sesé, and Fernando Luis

***Abstract*—We report the design and performance of thin-film microsusceptometers intended for magnetic measurements on samples at variable temperature down to the low mK range and excitation frequencies of up to about 1 MHz. The devices are realized as first-order gradiometers with two circular loops of 60 µm or 30 µm average diameter resulting in a total inductance of 360 pH or 250 pH, respectively. An integrated excitation coil generates a magnetic field with a transfer coefficient of 0.1 T/A at the sample position, whereas the Josephson junctions are located in a field-reduced area. The susceptometers are fabricated by a conventional Nb/AlOx/Nb trilayer process. In order to enhance the sensitivity to the level required for the measurement of sub-µm samples, an extra detection loop of 450 nm inner diameter was integrated into one of the pickup loops by using a focused ion beam (FIB). We show that this device is able of detecting signals from very small permalloy samples. An optimized susceptometer design with a predicted SQUID inductance of 12 pH is also presented, that can achieve an equivalent spin noise of 8 $\mu_B/\sqrt{\text{Hz}}$ at 4.2 K (μ_B is the Bohr magneton) when being equipped with a nanoloop of 100 nm line width and separation.**

Keywords*—Focused ion beam (FIB); microsusceptometer; nanoloop; permalloy; superconducting quantum interference device (SQUID)

I. Introduction

Superconducting quantum interference devices (SQUIDs) are sensitive detectors for weak magnetic signals. Commonly, they are designed with microscale dimensions and fabricated using well-established, reliable multilayer thin-film processes. The voltage-vs.-flux characteristic is a periodic function with the period being the flux quantum $\Phi_0 = 2.068\times10^{-15}$ Vs. A feedback coil is integrated into the device in order to operate it in a flux-locked loop (FLL) that linearizes the transfer function. The inductance of the SQUID loop is typically around $L \approx 100$ pH which results in low flux noise levels of about 1 $\mu\Phi_0/\sqrt{\text{Hz}}$. At low frequencies, usually below 10 Hz, $1/f$ excess noise is observed.

The growing interest in the investigation of nanoscale samples stimulated the development of so-called nanoSQUIDs, i.e., devices with overall loop dimension in the sub-µm regime (see, e.g., [1] and references therein). There are two basic benefits from the down-scaling of the device dimensions: (1) the coupling between sample and sensing loop is improved, and (2) the inductance of the SQUID ring and the capacitance of the Josephson junctions are lowered to $L < 1$ pH and $C < 0.1$ pF, respectively. Theoretically, with such low values of L and C, flux noise levels of the order of 10 $n\Phi_0/\sqrt{\text{Hz}}$ should be possible at $T = 4.2$ K. Unfortunately, due to limitations in junction fabrication, the best noise levels of today's nanoSQUIDs are much higher, 0.2 $\mu\Phi_0/\sqrt{\text{Hz}}$ with $1/f$ corner frequencies above 10 Hz [2], [3]. It is interesting to note that the same white noise levels are achieved at 4.2 K both with conventional SQUIDs if the inductance is reduced to about 10 pH [4] and with SQUIDs read out in a dispersive mode [5]. Furthermore, it is difficult to achieve a good coupling between a feedback coil and a sub-µm loop [6] for which reason nanoSQUIDs are mostly not equipped with a feedback coil. The remaining main benefits of nanoSQUIDs are their good coupling to nanoscale samples and their ability for operation in high magnetic fields. In this paper, we describe how SQUIDs fabricated in conventional technology can be upgraded by a single nanopatterning step to compete with the performance of nanoSQUIDs.

II. Basic Concept

The basic idea is illustrated in Fig. 1 by three representative pickup loop configurations labeled A-C. Loop A exhibits a minimum line width and spacing of 1.5 µm; it can thus be fabricated with conventional optical lithography. In case B, a quasi-circular nanoloop (approximated by a regular octagon) is added by removing material from the microloop. This nanoloop is connected in series to the microloop. An inner diameter of 300 nm and a minimum line width and spacing of 100 nm are assumed, which require advanced patterning techniques. As shown in case C, the dimension of the nanoloop can be further reduced, resulting in a narrow end piece shaped like loop A but with a minimized gap of 100 nm instead of 1.5 µm.

For a practical susceptometer, two series-connected pickup loops are wired as a first-order gradiometer in order to minimize the output signal without sample [7]-[9]. The net

Manuscript received December 14, 2013; accepted March 5, 2014.

This work was partly funded by the European Microkelvin Collaboration within the 7th Framework Programme of the European Commission (Grant number 228464), by the Spanish Ministry of Economy and Competitiveness (Grant MAT2012-38318-C03), and by the EMRP (EMRP: European Metrology Research Programme) project MetNEMS NEW08. The EMRP is jointly funded by the EMRP participating countries within EURAMET and the European Union.

D. Drung, J.-H. Storm, F. Ruede, A. Kirste, M. Regin, and T. Schurig are with the Physikalisch-Technische Bundesanstalt (PTB), 10587 Berlin, Germany (phone: +49-30-3481-7342; fax: +49-30-3481-69-7342; e-mail: dietmar.drung@ptb.de).

A. M. Repollés and F. Luis are with the Instituto de Ciencia de Materiales de Aragón, CSIC-Universidad de Zaragoza, and with the Departamento de Física de la Materia Condensada, Universidad de Zaragoza, 50009 Zaragoza, Spain.

J. Sesé is with the Instituto de Nanociencia de Aragón, and Laboratorio de Microscopias Avanzadas, Universidad de Zaragoza, 50018 Zaragoza, Spain.

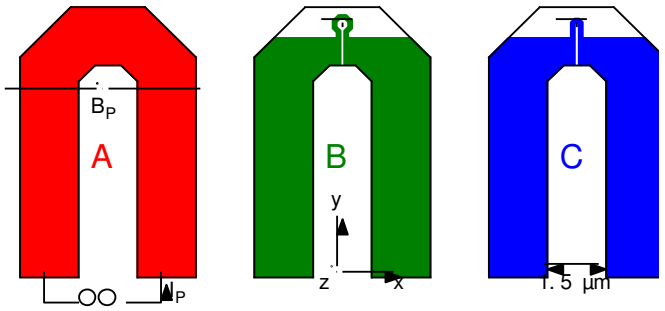

Fig. 1. Basic pickup loop structures. Panel A shows a microscale coplanar line with octagonal end cap, whereas in B and C nanoscale loops are integrated into the microscale structure. A minimum line width and spacing of 1.5 µm (case A) or 100 nm (cases B and C) are assumed, respectively. Horizontal lines through the pickup coil centers indicate the scans of the current-to-field calculation shown in Fig. 2. The coordinate system is placed on the symmetry axis of the structures as exemplarily shown for case B.

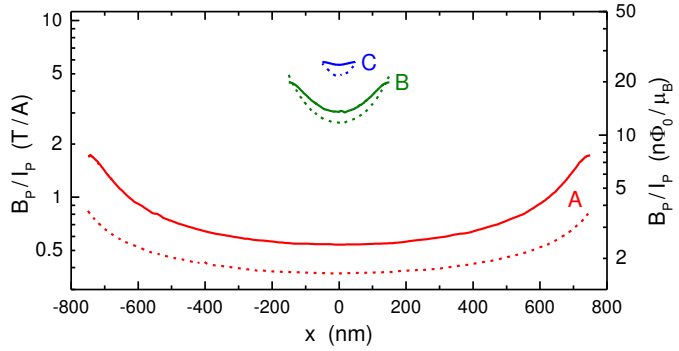

Fig. 2. Simulated transfer coefficient B_P/I_P for the three structures A-C depicted in Fig. 1. The superconductor is approximated by a perfect diamagnet with a London penetration depth $\lambda_L = 0$ (solid lines) or by a normal conductor (dashed lines). A film thickness of 100 nm is assumed. The magnetic field is calculated along the horizontal lines in Fig. 1 at a height $z = 50$ nm above the substrate surface; here, due to symmetry, B_P has a z-component only.

magnetic flux Φ in the SQUID is the sum of the fluxes in both pickup loops. To determine the SQUID's sensitivity to nanoscale samples, we calculate the total flux that a point-like magnetic dipole of magnetic moment µ couples to the nearby pickup loop L_P. The dipole is assumed as a planar current loop of current I and area A resulting in $\mu = IA$ and hence $\Phi = MI = M\mu/A$ (M is the mutual inductance between the current loop and L_P). Using the Lorentz reciprocity theorem, which states that sources and fields can be interchanged, the flux $B_P A = M I_P$ can be related to the magnetic dipole. Here, I_P is a current circulating through the pickup loop, B_P is the flux density generated by I_P at the dipole position, and the vectors of B_P and µ are oriented in the same direction for maximum coupling. By combining the above equations one obtains

$$\Phi = \mu \, B_P/I_P \, . \qquad (1)$$

Equation (1) shows that the transfer coefficient B_P/I_P is a figure of merit for the coupling between a magnetic dipole and the pickup loop. It may be specified in units of T/A or Φ_0/μ_B where $\mu_B = 9.274\times10^{-24}$ Am^2 is the Bohr magneton.

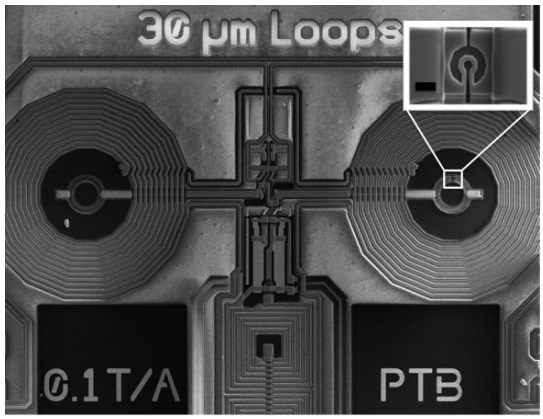

Fig. 3. SEM picture of a microsusceptometer consisting of two 30 µm loops, each of them surrounded by an 11-turn field coil. The center-to-center separation between the loops (baseline) is 350 µm. A magnified image is included showing the area where the nanoloop was fabricated; the scale bar is 1 µm.

To demonstrate the gain of the nanoloop, we simulated B_P/I_P for the three cases in Fig. 1 using the COMSOL Multiphysics® finite element program package. To simplify the simulation, we have considered two approximations for the Nb thin-film: ideal diamagnet with zero London penetration depth λ_L or normal conductor. For the nanoloops B and C in Fig. 1 the deviations between these two cases are quite moderate, i.e., the "true" result will depend only weakly on λ_L (cf. Fig. 2). In contrast, for the microscale pickup loop A the normal conductor approximation significantly underestimates the magnetic field because screening currents in the wide Nb film strongly affect the current distribution. Due to the large loop dimensions as compared to the penetration depth λ_L, the approximation $\lambda_L = 0$ is expected to yield realistic results if the distance between sample and coil edge is larger than a few λ_L. With a sample near the coil center, a roughly ten-fold improvement in B_P/I_P is predicted for the smallest nanoloop C compared to loop A.

III. Experimental Verification

To verify the predictions, the circuit line of one of the loops in a susceptometer was modified using a 48 pA focused beam of Ga^+ ions (FIB) in a Dual-Beam Helios NanoLab™ 600 system from FEI. As a result, we obtained a nanoloop with an inner diameter of ≈450 nm and a line width of ≈250 nm (see inset in Fig. 3). The thickness of the bottom Nb was ≈250 nm.

We measured the main characteristics of the SQUID susceptometer (current-voltage and voltage-flux curves, noise) before and after performing the FIB lithography, without noticing any appreciable changes. We only observed a small (0.4%) change in the mutual inductance imbalance of the two pickup loops with respect to the excitation coils, due to the removal of some superconducting material.

In order to fabricate a sufficiently small test sample, we deposited, using electron-beam evaporation, a 125 nm thick permalloy layer on a 50 nm PELCO® silicon nitride support film, commonly used for the preparation of transmission electron microscopy samples. Then a small piece of this

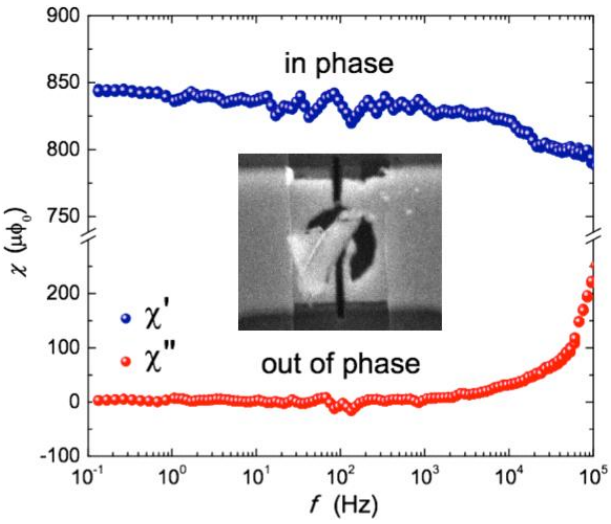

Fig. 4. In-phase and out-of-phase output signals of a SQUID susceptometer with nanoloop coupled to a permalloy sample, as shown in the inset. The output signal of the empty susceptometer has been subtracted. An ac current of 2.5 mA rms was applied to the excitation coil, which generates a magnetic flux density of 250 μT rms in the pickup loops.

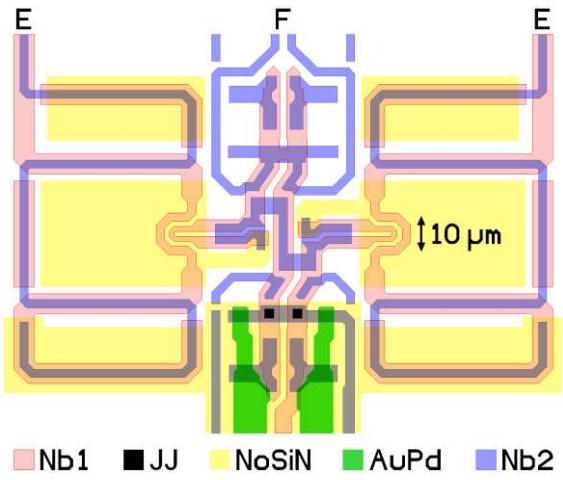

Fig. 5. Design of the miniaturized microsusceptometer (type SN) intended for equipment with a nanoloop. The center part of the existing susceptometers was taken nearly unmodified, but the large 11-turn excitation coils were replaced by small single-turn current loops. The minimum line width is 2.5 μm except for the pickup loop where 1.5 μm wide Nb1 lines are used. The layer NoSiN defines holes in the Si_xN_y insulation between Nb1 and Nb2. The contacts of feedback and excitation coils are marked by F and E, respectively.

sample was cut with the FIB and moved close to the nanoloop using an Omniprobe manipulator working inside the Helios 600 and monitored by SEM.

Fig. 4 shows the result of the test sample measurement performed at 4.2 K. The signal arising from the sample was obtained by subtracting the output of the empty susceptometer, which had been measured previously under identical conditions. The in-phase signal χ' shows a weak, close to logarithmic, dependence on frequency below 10 kHz, with a partial roll-off above this frequency. In agreement with Kramers-Kronig relations, the out-of-phase signal χ" increases with frequency. This behavior has been observed for other soft magnetic materials, such as Co based amorphous alloys [10]. It reflects the existence of a variety of magnetic relaxation processes, giving rise to a broad distribution of relaxation times. In nanometer-thick permalloy disks with diameters ranging from 100 nm to 1-2 microns, i.e., close to the dimensions of the sample used in the present experiments, such processes are associated with the depinning, either by thermal activation [11] or quantum tunneling [12], of a magnetic vortex [13,14]. The device reported in this work provides then, because of its geometry and enhanced sensitivity, a unique tool for directly measuring the vortex core transverse magnetization dynamics of individual soft magnetic disks, within a very broad frequency range and down to very low temperatures.

IV. Improved Susceptometer Design

Stimulated by the promising experimental results, we designed two miniaturized susceptometers intended for nanoloop integration. The basic characteristics of the new types SN and SU are summarized in Table I along with those of the existing types SM and SS. A common feature of the susceptometers is that the pickup loops L_P are directly forming the SQUID loop. Except for type SU, a separate feedback loop L_F is connected in series to the pickup loops for applying a feedback flux. The separation of feedback and pickup loops ensures that the feedback flux does not affect the magnetic field at the sample position. The total SQUID inductance is given by

$$L = 2\,(L_P + L_F + L_S) \qquad (2)$$

where L_S is the stray inductance of one half of the symmetric SQUID. Note that a second dummy inductance L_F has to be added for maximal symmetry/balance.

The first of the miniaturized devices (type SN) is basically a further development of our previous susceptometers (cf. Figs. 3 and 5). The center part is adopted nearly unmodified, but the large pickup loops are shrunk to a minimum (1.5 μm line width and spacing with our optical lithography), and the 11-turn excitation coils are replaced by single Nb1 lines closely surrounding the pickup loops. As both excitation and pickup loops are implemented in the same layer, effects from mask

TABLE I. Nominal Susceptometer Characteristics at 4.2 K

PTB type (main category)	*SM*	*SS*	*SN*	*SU*
Average pickup loop diameter, d_P (μm)	60	30	3	3
Pickup loop line width, w_P (μm)	6	3	1.5	1.5
Excitation coil constant, B_E/I_E (T/A)	0.1	0.1	0.06[a]	0.1[a]
Feedback coil sensitivity, $1/M_F$ (mA/Φ_0)	0.6	0.6	0.6	6.4
Pickup loop inductance, L_P (pH)	120	60	5	3
Feedback loop inductance, L_F (pH)	10	10	10	0
Stray inductance per SQUID half, L_S (pH)	50	55	10	3
Total SQUID inductance, L (pH)	360	250	50[a]	12[a]
Flux noise in 2stage setup, $\sqrt{S_\Phi}$ (μΦ_0/√Hz)	2	1.5	0.5[a]	0.2[a]

[a] Predicted performance without nanoloop.

misalignment are suppressed. Due to the minimal gap between the lines, a relatively high excitation coil sensitivity B_E/I_E of about 0.06 T/A is achieved. The excitation coil is designed as a second-order gradiometer such that the magnetic stray field has a zero-crossing at the position of the Josephson junctions (JJs). The coplanar Nb1 interconnect lines are covered with Nb2 plates (separated by the Si_xN_y isolation layer) in order to lower the stray inductance contribution L_S. The high-field region near the sample was kept free from covers to minimize excitation field distortion and to reduce problems with flux jumps at high fields [4]. The susceptometer is integrated on a 3.3 mm × 3.3 mm chip together with a 16-SQUID series array for readout in a two-stage (2stage) configuration [15]. The noise levels quoted in Table I include the contributions from the SQUID array and the room temperature FLL electronics [16].

V. Concept For Minimum SQUID Inductance

With the susceptometer design SN and our current fabrication process, a SQUID inductance $L \approx 50$ pH and a flux noise $\sqrt{S_\Phi} \approx 0.5\ \mu\Phi_0/\sqrt{\text{Hz}}$ are practical lower limits. To obtain a substantially lower noise of 0.2 $\mu\Phi_0/\sqrt{\text{Hz}}$, we developed a new susceptometer design SU based on our microSQUIDs (cf. Table I) [4]. These microSQUIDs are realized as first-order series gradiometers like the susceptometers. They have a minimized SQUID inductance $L \approx 10$ pH, but just one weakly coupled, quarter-turn coupling coil on each washer. Although it is possible in principle to apply both feedback flux and excitation field via the same coils, it is preferable in practice to have the coupling coils isolated from each other (in particular at high excitation frequencies).

In order to couple two galvanically isolated coils to each pickup loop with a sufficiently high mutual inductance, we introduce a separate coupling transformer. The corresponding layout and equivalent circuit are depicted in Figs. 6 and 7, respectively. Both the feedback current I_{F1} and excitation current I_E are passed through the single-turn primaries of the coupling transformer (right side in Fig. 6). The secondary of the coupling transformer is directly connected to a segment of the pickup loop. The screening current I_{C1} flows through this segment thereby creating a flux in the SQUID. The other coupling transformer (not depicted in Fig. 6 for clarity) is identically constructed. With this concept, as many coils as required can be efficiently coupled to a small pickup loop without increasing the SQUID inductance by a contribution L_F as for the devices described in the previous section.

There are several details considered in the new design. As for the previous devices, there is no material other than bottom Nb in the area intended for nanoloop patterning. The net stray fields of coupling transformers and pickup loops partially cancel at the location of the Josephson junctions. The 55 pH secondary inductance of the coupling transformer is much higher than the 0.5-1.5 pH segment of the pickup coil to which it is connected (cf. Fig. 7). This prevents a noticeable loss in sensitivity caused by the parallel connection of the two inductors. The area of the coupling washer is kept small in order to minimize screening currents from applied magnetic fields. For example, the 50 μT Earth field will cause a tolerable screening current of about 0.7 mA.

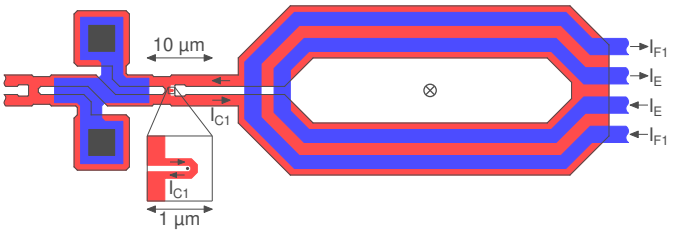

Fig. 6. Design concept for achieving a minimum SQUID inductance. For clarity, only the two Nb layers (red and blue) and the Josephson junctions (black) are shown. Details like shunt resistors, interconnect lines and holes in the insulation layer are omitted. The device is drawn to scale, with a tenfold magnification of the nanoloop region. Only one of the two coupling transformers is depicted.

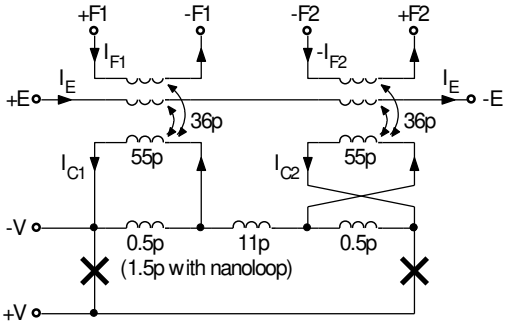

Fig. 7. Basic equivalent circuit for the design shown in Fig. 6. Crosses indicate the resistively shunted Josephson junctions. The quoted self and mutual inductances are estimated from the layout. The contact pads are labeled with ±V, ±E and ±F1/2 according to the terminology used for our other SQUID sensors.

Finally we note that, in contrast to the previous designs, the excitation field is not relatively homogeneous over the pickup loop because it is generated by a screening current through the circuit line of the loop. The maximum excitation field is determined by the critical current of this line. If a nanoloop is patterned into the pickup loop, the critical current decreases but the transfer coefficient B_P/I_{C1} increases (cf. Fig. 2). Therefore, the maximum excitation field depends only weakly on the size of the nanoloop. The imbalance caused by the inductance contribution of the nanoloop (about 1 pH for 100 nm structure size) may be canceled by passing an appropriate fraction of the excitation current through the spare feedback coil of this loop. Alternatively, nanoloops may be patterned into both pickup loops to keep symmetry.

VI. Conclusion

We have presented a scheme for integrating a nanoscale pickup loop into a microscale SQUID. This combination takes advantage of the high reliability and reproducibility of modern trilayer SQUID fabrication. For the susceptometer with the lowest SQUID inductance, $L \approx 12$ pH, a flux noise level of 0.2 $\mu\Phi_0/\sqrt{\text{Hz}}$ is predicted at 4.2 K comparable with today's best nanoSQUIDs. By patterning a nanoloop of 100 nm minimum line width and spacing into the pickup loop, transfer coefficients of up to 25 $n\Phi_0/\mu_B$ can be obtained, which allows for a very low equivalent spin noise down to 8 $\mu_B/\sqrt{\text{Hz}}$ at 4.2 K. The

noise level could be further improved by using smaller Josephson junctions, which also reduces the effect of the excitation field on the junctions [3], [17]. Another option is cooling the devices to mK temperatures. For our SQUIDs, the noise levels off below about 300 mK, yielding a minimum rms noise of ≈30% of the 4.2 K value. For the 12 pH susceptometer we expect a minimum flux noise of 60 $n\Phi_0/\sqrt{Hz}$, a factor of two above the value recently reported for a SQUID with dispersive readout operated at 25 mK [18]. Combining low operation temperatures with sub-µm junctions could allow for an equivalent spin noise level of 1 $\mu_B/\sqrt{Hz}$. However, this approach is limited to high signal frequencies due to excess low-frequency noise typically observed at mK temperatures [19].

ACKNOWLEDGMENT

The authors thank S. Bechstein, M. Fleischer-Bartsch, and M. Klemm for susceptometer characterization, and C. Aßmann for helpful discussions on nanopatterning.

REFERENCES

[1] C. P. Foley and H. Hilgenkamp, "Why NanoSQUIDs are important: an introduction to the focus issue," Supercond. Sci. Technol., vol. 22 064001, June 2009.

[2] L. Hao, J. C. Macfarlane, J. C. Gallop, D. Cox, J. Beyer, D. Drung, and T. Schurig, "Measurement and noise performance of nano-superconducting-quantum-interference devices fabricated by focused ion beam," Appl. Phys. Lett., vol. 92, 192507, May 2008.

[3] R. Wölbing, J. Nagel, T. Schwarz, O. Kieler, T. Weimann, J. Kohlmann, A. B. Zorin, M. Kemmler, R. Kleiner, and D. Koelle, "Nb nano superconducting quantum interference devices with high spin sensitivity for operation in magnetic fields up to 0.5 T," Appl. Phys. Lett., vol. 102, 192601, May 2013.

[4] S. Bechstein, A. Kirste, D. Drung, M. Regin, O. Kazakova, J. Gallop, L. Hao, D. Cox, and T. Schurig, "Investigation of material effects with micro-sized SQUID sensors," IEEE Trans. Appl. Supercond., vol. 23, 1602004, June 2013.

[5] J.-M. Mol, J. Arps, F. Foroughi, G. W. Gibson, Jr., K. Fung, B. Klopfer, K. Nowack, P. A. Kratz, M. E. Huber, K. A. Moler, J. R. Kirtley, and H. Bluhm, "High-sensitivity SQUIDs with dispersive readout for scanning microscopy," Paper F4 at 14th International Superconductive Electronics Conference (ISEC), Cambridge, MA, USA, July 7-11, 2013.

[6] C. Granata, E. Esposito, A. Vettoliere, L. Petti and M. Russo, "An integrated superconductive magnetic nanosensor for high-sensitivity nanoscale application," Nanotechnology, vol. 19, 275501, July 2008.

[7] M. B. Ketchen, T. Kopley, and H. Ling, "Miniature SQUID susceptometer," Appl. Phys. Lett., vol. 44, pp. 1008–1010, May 1984.

[8] M. E. Huber, N. C. Koshnick, H. Bluhm, L. J. Archuleta, T. Azua, P. G. Björnsson, B. W. Gardner, S. T. Halloran, E. A. Lucero, and K. A. Moler, "Gradiometric micro-SQUID susceptometer for scanning measurements of mesoscopic samples," Rev. Sci. Instrum., vol. 79, 053704, May 2008.

[9] S. T. P. Boyd, V. Kotsubo, R. Cantor, A. Theodorou, and J. A. Hall, "Miniature thin-film SQUID susceptometer for magnetic microcalorimetry and thermometry," IEEE Trans. Appl. Supercond., vol. 19, pp. 697-701, June 2009.

[10] S. Vitale, R. Tommasini, M. Cerdonio, M. Bonaldi, A. Cavalleri, and G. Durin, "Magnetic viscosity, thermal relaxation, and thermal equilibrium noise in Co based amorphous alloys at milliKelvin temperatures," J. Appl. Phys., vol. 72, pp. 4820-4825, Nov. 1992.

[11] J. A. J. Burgess, D. C. Fortin, J. E. Losby, D. Grombacher, J. P. Davis, and M. R. Freeman, "Thermally activated decay of magnetic vortices," Phys. Rev. B, vol. 82, 144403, Oct. 2010.

[12] R. Zarzuela, S. Vélez, J. M. Hernández, J. Tejada, and V. Novosad, "Quantum depinning of the magnetic vortex state in micron-size permalloy disks," Phys. Rev. B, vol. 85, pp. 180401(R), May 2012.

[13] R. P. Cowburn, D. K. Koltsov, A. O. Adeyeye, M. E. Welland, and D. M. Tricker, "Single-domain circular nanomagnets," Phys. Rev. Lett., vol. 83, pp. 1042-1045, Aug. 1999.

[14] T. Shinjo, T. Okuno, R. Hassdorf, K. Shigeto, and T. Ono, "Magnetic vortex core observation in circular dots of permalloy," Science, vol. 289, pp. 930-932, Aug. 2000.

[15] D. Drung, C. Aßmann, J. Beyer, A. Kirste, M. Peters, F. Ruede, and T. Schurig, "Highly sensitive and easy-to-use SQUID sensors," IEEE Trans. Appl. Supercond., vol. 17, pp. 699-704, June 2007.

[16] http://www.magnicon.com/squid-electronics/xxf-1/

[17] S. Anders, M. Schmelz, L. Fritzsch, R. Stolz, V. Zakosarenko, T. Schönau and H.-G. Meyer, "Sub-micrometer-sized, cross-type Nb–AlOx–Nb tunnel junctions with low parasitic capacitance," Supercond. Sci. Technol., vol. 22, 064012, June 2009.

[18] E. M. Levenson-Falk, R. Vijay, N. Antler and I. Siddiqi, "A dispersive nanoSQUID magnetometer for ultra-low noise, high bandwidth flux detection," Supercond. Sci. Technol., vol. 26, 055015, May 2013.

[19] D. Drung, J. Beyer, J.-H. Storm, M. Peters, and T. Schurig,, "Investigation of low-frequency excess flux noise in dc SQUIDs at mK temperatures," IEEE Trans. Appl. Supercond., vol. 21, pp. 340–344, June 2011.